Pflügers Arch – Eur J Physiol (1999) 439:27–38
Digital Object Identifier (DOI) 10.1007/s004249900158

ORIGINAL ARTICLE

Matthias Bödding · Reinhold Penner

Differential modulation of voltage-dependent Ca^{2+} currents by EGTA and BAPTA in bovine adrenal chromaffin cells

Received: 15 March 1999 / Received after revision: 12 August 1999 / Accepted: 20 August 1999 / Published online: 13 October 1999

Abstract Whole-cell patch-clamp recordings were made to examine the effects of the Ca^{2+} chelators EGTA and BAPTA on the biophysical properties of voltage-operated Ca^{2+} currents in bovine adrenal chromaffin cells. Ca^{2+} currents in the presence of either EGTA or BAPTA over a concentration range of 0.1–60 mM were recorded under otherwise identical conditions. Analysis of current-voltage relationships yielded unexpected differences in several important parameters such as the voltage dependence of activation, kinetics, slope, and reversal potential, which seemed to be unrelated to the Ca^{2+}-binding properties of these chelators. Increasing concentrations of BAPTA augmented the peak Ca^{2+} current amplitude while current amplitudes in the presence of EGTA remained constant over the entire concentration range tested. Increasing concentrations of BAPTA shifted the voltage sensitivity of Ca^{2+} currents by about 15 mV towards positive voltages. EGTA, over the same concentration range, did not affect the voltage sensitivity. The shift in voltage sensitivity observed with BAPTA was unrelated to its faster Ca^{2+}-binding kinetics, as it was also observed when substituting Ca^{2+} with Ba^{2+} as the charge carrier. The mechanism by which BAPTA affects Ca^{2+} channel voltage dependence also seems unrelated to kinase-mediated modulation of Ca^{2+} channels, since the protein-kinase-C- (PKC-) specific drugs bisindolylmaleimide and phorbol ester (PMA) neither mimicked nor prevented the action of BAPTA. The less specific kinase inhibitor staurosporine, however, augmented Ca^{2+} currents similarly to BAPTA, but without affecting the voltage sensitivity. The BAPTA-mediated shift in voltage sensitivity was partially suppressed by non-hydrolysable analogs of GTP (GDP[β-*S*] and GTP[γ-*S*]). Lowering $[Mg^{2+}]_i$ mimicked the BAPTA-induced shift in voltage sensitivity and prevented further shifts in voltage sensitivity by BAPTA. The results demonstrate that BAPTA and EGTA, despite their similarities in terms of Ca^{2+} buffering, have disparate effects on the voltage dependence of Ca^{2+} channels and careful selection of the chelator is required to quantitatively assess Ca^{2+} currents.

Key words Ca^{2+} influx · Chelators · Chromaffin cells

M. Bödding · R. Penner
Department of Membrane Biophysics,
Max-Planck-Institute for Biophysical Chemistry,
Am Fassberg, D-37077 Göttingen, Germany

R. Penner (✉)
Queen's Medical Center Neuroscience Institute,
University of Hawaii, 1960 East-West Road, Honolulu,
HI 96822, USA
e-mail: rpenner@hawaii.edu
Tel.: +1-808-9565522, Fax: +1-808-9568713

Introduction

The Ca^{2+} chelators 1,2-bis-(*o*-aminophenoxy)-ethane-*N*,*N*,*N*',*N*'-tetraacetic acid (BAPTA) and ethyleneglycol-bis-(β-aminoethylether)-*N*,*N*,*N*',*N*'-tetraacetic acid (EGTA) are widely used tools in biological research. In electrophysiological measurements they are used as internal ingredients for various purposes, particularly when investigating Ca^{2+} currents, as they bind Ca^{2+} with high selectivity and affinity. As a result, they reduce Ca^{2+}-induced inactivation of Ca^{2+} currents produced by the incoming Ca^{2+}. In addition, the concentration gradient across the plasma membrane is kept steep to allow more Ca^{2+} to enter the cell, thus enabling investigators to record large and sustained Ca^{2+} currents without damaging cells due to Ca^{2+} overload. Furthermore, the effective suppression of elevations in intracellular Ca^{2+} concentration ($[Ca^{2+}]_i$) also suppresses Ca^{2+}-activated K^+ and Cl^- currents. Another use for these exogenous Ca^{2+} buffers is to clamp $[Ca^{2+}]_i$ to a desired level by appropriate mixtures of Ca^{2+} and buffer concentrations. Recently, BAPTA has replaced EGTA as the chelator of choice, because of its improved characteristics concerning pH sensitivity and speed in binding Ca^{2+} [35].

EGTA and BAPTA are normally used at millimolar concentrations, so it is possible that they might have additional effects other than chelating Ca^{2+}. Indeed, Hille and coworkers found that BAPTA interferes with the

muscarinic signal transduction pathway in rat sympathetic neurons. This chelator, but not EGTA, was found to block the muscarinic suppression of Ca^{2+} currents and this effect is independent of its Ca^{2+}-binding properties [5, 6, 7, 18]. Penner and Neher [29] showed that, in rat peritoneal mast cells, exocytosis induced by guanosine 5'-*O*-(3-thiotriphosphate) (GTP[γ-*S*]) is inhibited by dibromo-BAPTA at 4 mM, while even higher concentrations of EGTA did not impede the actions of GTP[γ-*S*]. Furthermore, it was shown that Ca^{2+} chelators can directly interfere with proteins, e.g. inositol 1,4,5-trisphosphate (IP_3) receptors [23, 31] or protein kinases [9], pointing towards possible pharmacological effects of these buffers. In a more recent study Parekh and Penner [26] proposed a blocking effect of BAPTA on protein kinase C (PKC) in rat basophilic leukemia cells. In these cells, BAPTA prevents the PKC-mediated inactivation of a store-operated Ca^{2+} current, while EGTA does not. Therefore, it is fundamentally important to test whether these Ca^{2+} chelators, which are generally used for enhancing Ca^{2+} currents, interfere with them pharmacologically or otherwise.

This issue was addressed in whole-cell patch-clamp recordings from bovine adrenal chromaffin cells. The two chelators EGTA and BAPTA had strikingly different effects on the biophysical characteristics of voltage-operated Ca^{2+} currents with respect to magnitude, voltage dependence, kinetics and selectivity. In particular, BAPTA induced significant changes in the voltage sensitivity of Ca^{2+} channels and should therefore be used with caution when investigating voltage-dependent modulation of Ca^{2+} currents. A preliminary report of this work has been presented [8].

Materials and methods

Cell preparation

Bovine chromaffin cells were prepared essentially as described elsewhere [13, 22]. Briefly, Locke's Ca^{2+}-free buffer (154 mM NaCl, 5.6 mM KCl, 2.15 mM Na_2HPO_4, 0.85 mM NaH_2PO_4, 10 mM glucose, pH 7.0) containing 2–3 mg/ml collagenase A (Boehringer Mannheim) was injected into the vena suprarenalis of bovine adrenal glands. The exact collagenase concentration was empirically determined for each batch according to its activity (about 0.95 U/mg). Glands were transferred to a shaking bath for 10 min at 37°C after which the collagenase-containing Locke's solution in the glands was refreshed and glands were placed in the shaking bath for another 10 min. Then, the glands were sliced and the digested medulla was cut into small pieces. This tissue was triturated and filtered through a 50-µm diameter nylon mesh and rinsed with Locke's solution. The collected cell suspension was centrifuged twice at 158 *g* for 2 min. The pellet was resuspended in Locke's solution and purified on a Percoll gradient (LKB, Pharmacia, Freiburg, Germany) at 12°C for 20 min at 20,000 *g*. After removal of the light cell detritus, chromaffin cells were carefully separated from the blood cells underneath. Culture medium M199 supplemented with 80,000 U/l penicillin, 80 mg/l streptomycin and 10% fetal calf serum at pH 7.5 was added to the chromaffin cells, which were then centrifuged for 6 min at 227 *g* to remove remaining Percoll. After resuspension in the culture medium, cells were seeded on poly-L-lysine-coated coverslips and incubated at 37°C, 10% CO_2 at 90% humidity. Culture medium was changed 4–5 h after finishing the cell preparation and 2 days later. Cells were used for experiments on the second and third day after plating.

Solutions

To isolate Ca^{2+} or Ba^{2+} currents through voltage-dependent Ca^{2+} channels, Na^+ and K^+ conductances were eliminated by including tetrodotoxin (TTX) and tetraethylammonium chloride (TEA-Cl) in the bath solution and using *N*-methyl-D-glucamine instead of potassium in the internal solution. The external bath solution contained (in mM): 135 NaCl, 10 $CaCl_2$, 2.8 KCl, 2 $MgCl_2$, 11 glucose, 10 HEPES, 10 TEA-Cl, 0.01 TTX adjusted to pH 7.2 with NaOH. In some experiments equimolar Ba^{2+} was used instead of Ca^{2+} as the charge carrier. The patch-pipette solution contained (in mM): 150 *N*-methyl-D-glucamine chloride (NMG-Cl), 10 HEPES, 8 NaCl, 1 $MgCl_2$, 4 Mg-ATP, 0.3 Na_2-GTP adjusted to pH 7.2 with NaOH. The Ca^{2+} chelators EGTA and BAPTA were added to the intracellular solution at 0.1, 0.3, 1, 3, 10, 30 or 60 mM; both as tetracaesium salts. Stock solutions of 500 mM were prepared in water and the pH was adjusted to 7.2 with CsOH and HCl. When using high concentrations of Ca^{2+} chelators, the osmolarity was kept constant between internal and external solutions by appropriate reduction of $[NMG\text{-}Cl]_i$ or addition of sucrose to the external solution. No differences in the recorded Ca^{2+} currents were observed with either of these procedures. EGTA was obtained from Fluka (Buchs, Switzerland) and BAPTA (Lot 2841–2) was from Molecular Probes (Eugene, Ore., USA); according to manufacturers both at >99% purity. Staurosporine and 2-[1-(3-dimethylaminopropyl)-1*H*-indol-3-yl]-3-(1*H*-indol-3-yl)-maleimide (bisindolylmaleimide) were purchased from Calbiochem (Bad Soden, Germany). All other chemicals were from Sigma (Deisenhofen, Germany).

Electrophysiology

Membrane currents were measured with the patch-clamp technique in the tight-seal whole-cell configuration [15]. Single cells were voltage-clamped using a computer-controlled EPC-9 patch-clamp amplifier (HEKA, Lamprecht, Germany). Patch pipettes were made from borosilicate glass (Kimax, Vineland, N.Y., USA) and their tips fire-polished and coated with Sylgard. Pipette resistances were between 1.5 and 3 MΩ when filled with the standard internal solution. The series resistances were typically in the range of 4–10 MΩ and not electronically compensated. The seal resistances were usually above 5 GΩ. Currents were low-pass filtered at 8.8 kHz and digitized at 100-µs intervals. Recordings were usually started after 2–3 min following establishment of the whole-cell configuration to allow for diffusional equilibration of the buffers from the pipette into the cytosol [30]. Usually, about five ramps spanning from –100 mV to 100 mV in 50 ms were applied before the recording of the current-voltage relationships was started. Once the Ca^{2+} currents elicited by the ramp protocol remained constant, pulse depolarizations from a holding potential of –70 mV were applied. The depolarization length of each test pulse was typically 25 ms. Leak currents were corrected by a P/4 procedure. Cell capacitance was determined and compensated before each voltage pulse, using the automatic capacitance neutralization of the EPC-9 amplifier.

For each concentration of Ca^{2+} chelator tested, at least two different cell preparations were used. The membrane potential values given in this paper are corrected for liquid junction potentials (LJP), according to $V_c = V - LJP$, where V_c is the "true" (corrected) voltage, V the applied voltage (theoretical) voltage during a step depolarization, and LJP the liquid junction potential. LJPs for the various solutions were measured as described previously [24] and are listed in Table 1.

All experiments were carried out at room temperature (20–23°C). Data analysis was performed with PulseFit (HEKA, Lamprecht, Germany) and IGOR Pro (WaveMetrics, Lake Oswe-

Table 1 Liquid junction potentials (*LJP*) of internal solutions

Internal solution + chelator	Concentration (mM)	LJP (mV)*
BAPTA or EGTA	0.1	–4.0
	0.3	–3.5
	1	–3.0
	3	–2.0
	10	0.3
	30	2.0
	60	5.5
10 mM $MgCl_2$ + BAPTA	1	–4.9
	60	3.7
0 mM $MgCl_2$ + BAPTA	1	–4.1
	60	4.7
0.5 mM EDTA + BAPTA	1	–3.5
	60	5.2
1 mM EDTA	1	–1.9
(4 mM Na_2ATP) + BAPTA	60	5.3

*LJP were measured against the standard external Ringer solution

go, USA) software packages. The free Ca^{2+} and Mg^{2+} concentrations were calculated by custom software using stability constants given by Martell and Smith [21]. Data points for the current-voltage curves were obtained by taking the average amplitude of the last 20% at the end of each test pulse. The current-voltage relationships of Ca^{2+} currents were fitted with a Boltzmann function, a linear term and a term for positive block according to:

$$I_{Ca}=g_{max}\times(V_m-E_{rev})\times(1/\{1+\exp[-(V_m-V_{1/2}/slope]\})\times(1/\{1+\exp[-(V_m-V_{1/2\,block}/slope_{block})]\})$$

where g_{max} is the maximal conductance, V_m the test potential, E_{rev} the reversal potential and $V_{1/2}$ the voltage of half-maximal activation. Throughout, average data are given as means ±SEM for n number of cells. Student's paired t-test was used to assess statistical significance.

Results

Whole-cell patch-clamp recordings were made to examine possible effects of Ca^{2+} chelators on voltage-operated Ca^{2+} currents in bovine adrenal chromaffin cells. For this purpose, current-voltage relationships of Ca^{2+} currents were recorded by using 0.1, 0.3, 1, 3, 10, 30 and 60 mM of either EGTA or BAPTA in the standard internal solution. This covers the entire practical range of concentrations routinely used by electrophysiologists.

Effects of BAPTA and EGTA on current-voltage relationships

In chromaffin cells, typical Ca^{2+} currents were evoked by step depolarizations to various membrane voltages as illustrated in Fig. 1A. The average current-voltage relationships for Ca^{2+} currents in the presence of 1, 30 or 60 mM EGTA in the intracellular solution are shown in Fig. 1B. The three current-voltage curves display similar voltage dependence and vary only slightly in their peak current amplitudes. However, when using the same concentrations of BAPTA instead of EGTA, the current-voltage curves reveal obvious differences (Fig. 1C), suggesting that BAPTA can alter the current-voltage sensitivity of Ca^{2+} channels. Increasing concentrations of BAPTA from 1, 30 and 60 mM shifted the current-voltage curves to more positive voltages. Furthermore the maximal current was increased at 30 mM BAPTA but decreased at 60 mM BAPTA.

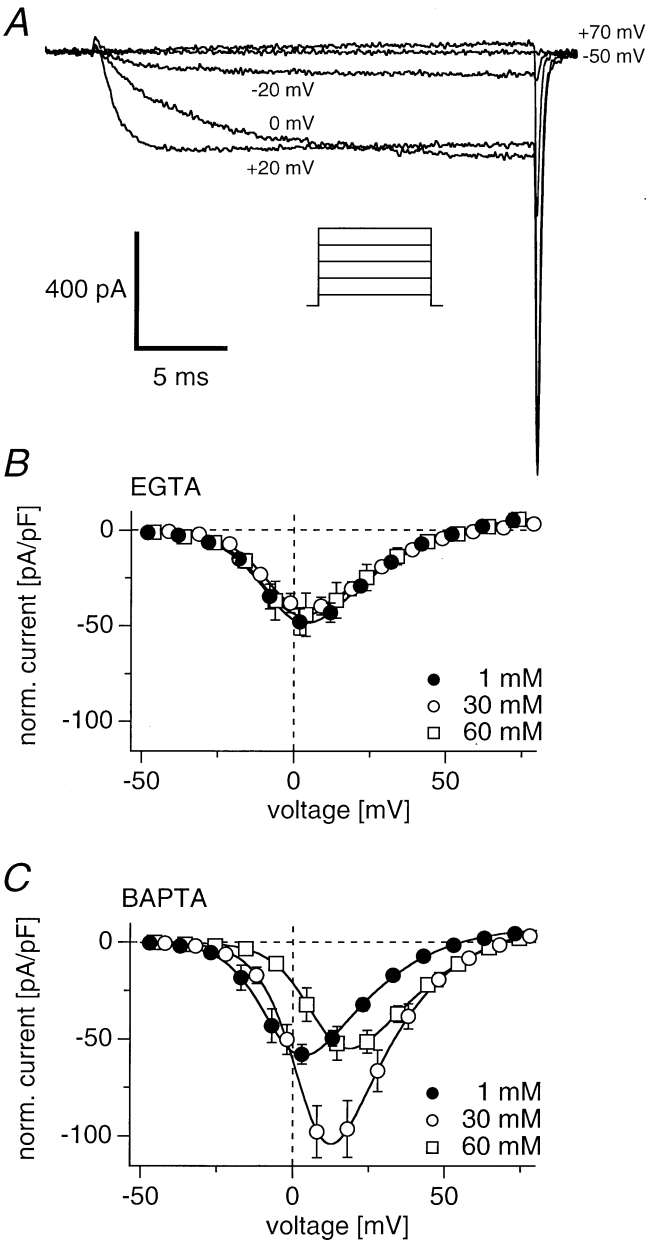

Fig. 1A–C Effects of EGTA and BAPTA on current-voltage relationships for Ca^{2+} currents. **A** Representative high-resolution Ca^{2+} currents evoked by stepwise depolarizations to the voltages indicated in the *graph*. Currents were recorded with the standard extracellular and intracellular solutions with 10 mM EGTA in the pipette solution. **B** Average current-voltage relationship taken from cells perfused with standard internal solution supplemented with either 1 mM (●; n=4), 30 mM (○; n=4), or 60 mM EGTA (□; n=5). **C** Average current-voltage relationship taken from cells perfused with either 1 mM (●; n=7), 30 mM (○; n=6) or 60 mM BAPTA (□; n=8)

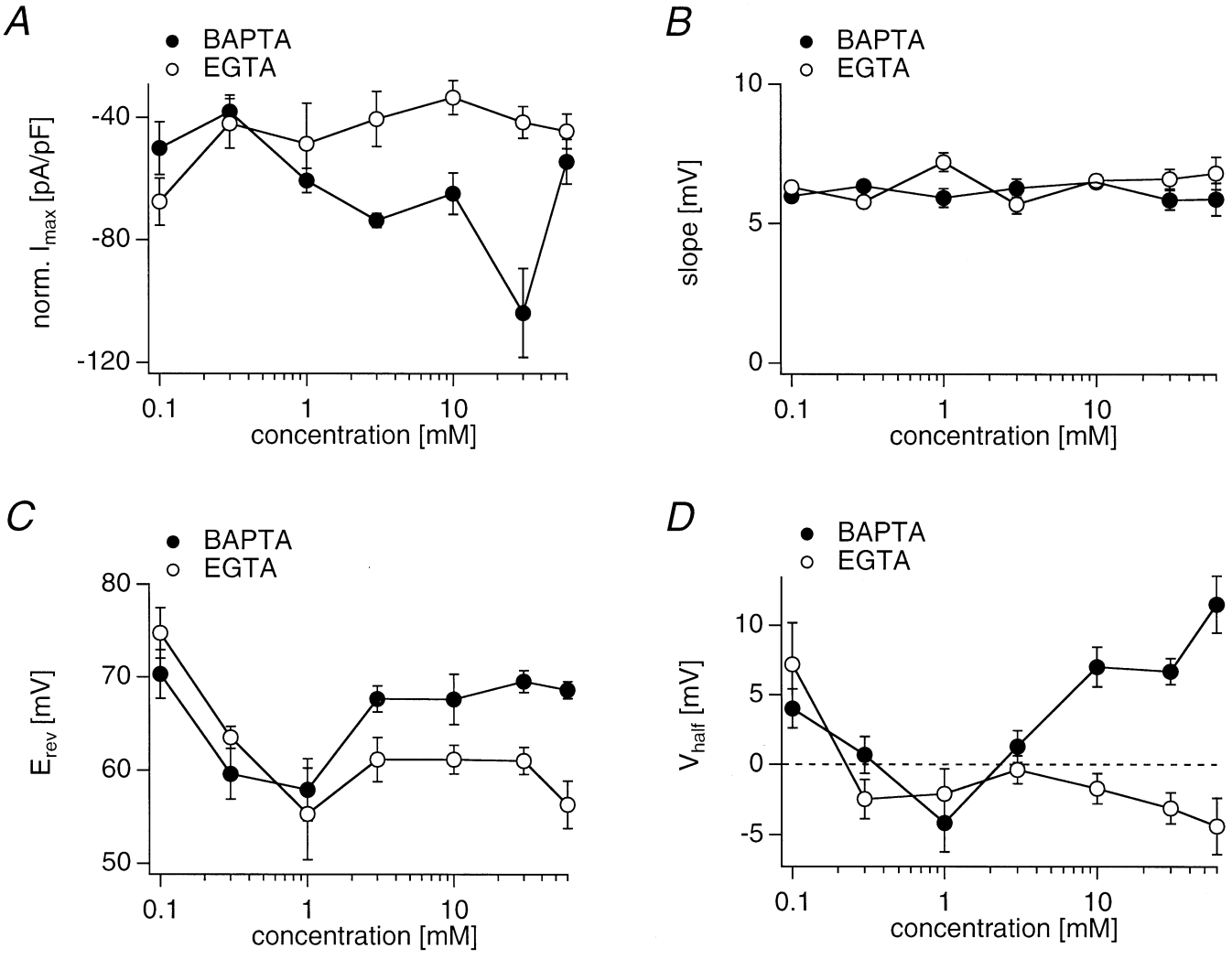

Fig. 2A–D Effects of BAPTA or EGTA on biophysical parameters derived from current-voltage curves. All parameters were obtained by best fits to current-voltage curves according to the formula described in Materials and methods. **A** Effects of BAPTA (●; n=4–7) or EGTA (○; n=4–8) on mean I_{max} depending on chelator concentration. I_{max} was taken as the peak current of each current-voltage curve. **B** Effects of BAPTA (●; n=4–7) or EGTA (○; n=4–8) on the mean slope value as a function of chelator concentration. **C** Effects of BAPTA (●; n=4–7) or EGTA (○; n=4–8) on the mean reversal potential (E_{rev}) depending on chelator concentration. **D** Effects of BAPTA (●; n=4–7) or EGTA (○; n=4–8) on the mean half-maximal activation voltage (V_{half}) as a function of chelator concentration

To further investigate these unexpected differences of the two commonly used Ca^{2+} chelators on voltage-operated Ca^{2+} currents, we analysed the fundamental biophysical current-voltage parameters I_{max}, V_{half}, slope and E_{rev} for the entire concentration range (summarized in Fig. 2 and Table 2).

The peak Ca^{2+} current amplitude is influenced by several factors. For example, an increase in Ca^{2+} influx might decrease Ca^{2+} currents by negative feedback inhibition through Ca^{2+}-induced inactivation, which is due to direct binding of Ca^{2+} at the inner pore region of Ca^{2+} channels [36]. Such Ca^{2+}-induced inactivation is particularly prominent in L-type channels and less so in other types of voltage-dependent Ca^{2+} channels. Since bovine chromaffin cells mainly express N-, P- and Q-type Ca^{2+} channels and few L-type channels [1, 2, 3], we observed little effect of increasing levels of EGTA on whole-cell Ca^{2+} current amplitude. Over the range of 0.3–60 mM EGTA, the current size normalized to cell capacitance remained fairly constant around –40 pA/pF (Fig. 2A). Only at 0.1 mM EGTA was the current density unexpectedly higher (–68±9 pA/pF, n=6). It remains to be determined what the reason for this apparent potentiation is and whether it is due to Ca^{2+}-dependent potentiation of Ca^{2+} currents as reported for other cell types [28]. When using the chelator BAPTA, the peak current amplitudes were larger compared to EGTA, particularly at concentrations above 1 mM. Current size increased from 0.3 to 30 mM BAPTA. The maximal current amplitude was –104± 5 pA/pF at 30 mM BAPTA and with 60 mM BAPTA the amplitude decreased again to –55±6 pA/pF. With little added chelator (0.1–0.3 mM BAPTA), the normalized Ca^{2+} currents were estimated to be –50±8 pA/pF and –38±8 pA/pF, respectively, which are comparable to the values recorded with EGTA.

Table 2 Effects of chelators on current-voltage parameters of Ca^{2+} currents

Chelator	Concentration (mM)	V_{half} (mV)	Slope (mV)	E_{rev} (mV)	I_{max} (pA/pF)	*n*
EGTA	0.1	7.2±3.0	6.3±0.2	74.7±2.7	–67.7±8.7	6
	0.3	–2.5±1.4	5.8±0.0	63.5±1.2	–42.0±5.4	5
	1	–2.1±1.8	7.2±0.3	55.3±4.9	–48.7±4.0	4
	3	–0.4±1.0	5.7±0.3	61.1±2.4	–40.6±2.2	6
	10	–1.7±1.1	6.5±0.2	61.1±1.5	–33.6±6.8	7
	30	–3.1±1.1	6.6±0.4	61.0±1.4	–41.6±14.4	4
	60	–4.4±2.0	6.8±0.6	56.3±2.5	–44.6±7.4	5
BAPTA	0.1	4.0±1.4	6.0±0.2	70.3±2.6	–50.1±7.8	4
	0.3	0.7±1.3	6.3±0.2	59.6±2.7	–38.2±8.1	4
	1	–4.2±2.1	5.6±0.1	57.9±3.3	–60.8±13.3	7
	3	1.3±1.1	6.3±0.2	67.7±1.4	–73.8±9.1	5
	10	7.0±1.4	6.5±0.2	67.6±2.7	–65.0±5.5	7
	30	6.7±0.9	5.8±0.3	69.5±1.2	–103.8±5.2	6
	60	11.5±2.1	5.9±0.2	58.6±0.9	–55.1±5.7	8

All values are means ±SEM. Values represent averaged parameters derived from fits to current-voltage relationships of individual cells

The slope of the current-voltage curves was measured to arrive at an estimate of the gating sensitivity with which the Ca^{2+} channels open. For all EGTA concentrations, the slope was constant at about 6 mV (Fig. 2C). Therefore, the sensitivity of the channels' switch to the open state seemed unaffected by the EGTA concentrations tested. Similarly, with BAPTA, the slopes of the activation curves also remained constant at a value of around 6.5 mV (Fig. 2B).

E_{rev} was estimated, to assess the selectivity of the Ca^{2+} channels. In the concentration range of 1 to 60 mM EGTA, E_{rev} was at about +60 mV (Fig. 2C). With BAPTA, the reversal potentials also remained stable (at about 68 mV) over the concentration range of 3–60 mM. At concentrations below 1 mM of either chelator species, E_{rev} slightly increased from values around +60 mV to about +70 mV (Fig. 2C). Thus, the Ca^{2+} selectivity of the Ca^{2+} channels was similar over a wide concentration range. The slightly lower apparent selectivity at higher buffer concentrations might stem from the somewhat higher Cs^+ permeability of Ca^{2+} channels at very low intracellular Ca^{2+} levels and the relative increase in internal Cs^+ (chelators were used as tetracaesium salts).

V_{half} indicates the voltage at which half-maximal activation of the Ca^{2+} channels occurs. This parameter was of particular interest, because a shift in V_{half} would reflect a change in the channels' voltage sensitivity. Again, over the concentration range of 0.3–60 mM EGTA, this parameter was fairly stable at about –2 mV (Fig. 2D). With 0.1 mM EGTA, V_{half} was 7±3 mV and might be related to Ca^{2+}-dependent inhibition of Ca^{2+} channel gating by intracellular Ca^{2+}. On the other hand, BAPTA exhibited a prominent effect on this current-voltage parameter. V_{half} increased from –4±2 mV at 1 mM to 12±2 mV at 60 mM (significant at $P<0.05$). Thus, in contrast to EGTA, BAPTA shifted the current-voltage curves by about 16 mV in the depolarizing direction (Fig. 2D).

Effects of BAPTA and EGTA on Ca^{2+} current kinetics

To investigate whether the effects of the two chelators on the current-voltage relationship were mirrored in the activation time constants, we analysed the activation kinetics of the Ca^{2+} currents in the presence of the various buffers. This allowed us to distinguish between the kinetic- and voltage-dependent effects of the buffers.

The activation time constants for 1, 30 and 60 mM EGTA are shown in Fig. 3A. In agreement with previous data, EGTA did not affect the kinetics of Ca^{2+} currents. However, with increasing concentrations of BAPTA, the activation time constants of Ca^{2+} currents became less (Fig. 3B), presumably reflecting the altered voltage sensitivity of Ca^{2+} channels. Indeed, when shifting the time constants for the 1 mM BAPTA concentration along the voltage axis by 15 mV in the depolarizing direction, one can match the values obtained for 60 mM BAPTA. This shift is almost identical to the one observed for the activation curve. Thus, the BAPTA-induced shift in the kinetics is probably caused by the shift in the voltage sensitivity of Ca^{2+} channels as described above and not a separate effect on channel kinetics.

Given the fact that BAPTA and EGTA affect Ca^{2+} currents differently and since the above experiments were carried out with Ca^{2+} as the charge carrier, the first question that needed to be addressed was whether the faster on-rate of Ca^{2+} binding to BAPTA might be responsible for the observed discrepancies. To this end, we tested whether the permeating ion through Ca^{2+} channels plays a role in the BAPTA-induced effects by substituting the physiological permeating Ca^{2+} by equimolar amounts of Ba^{2+}. With 1 or 60 mM $[BAPTA]_i$ and in the presence of 10 mM $BaCl_2$ in the external solution, the shift of the current-voltage curves remained obvious although reduced (see Table 3). This suggests that the BAPTA-induced shift in the current-voltage curves is not totally dependent on the charge carrier and that it must be mediated by mechanisms in addition to Ca^{2+} entering through the channels.

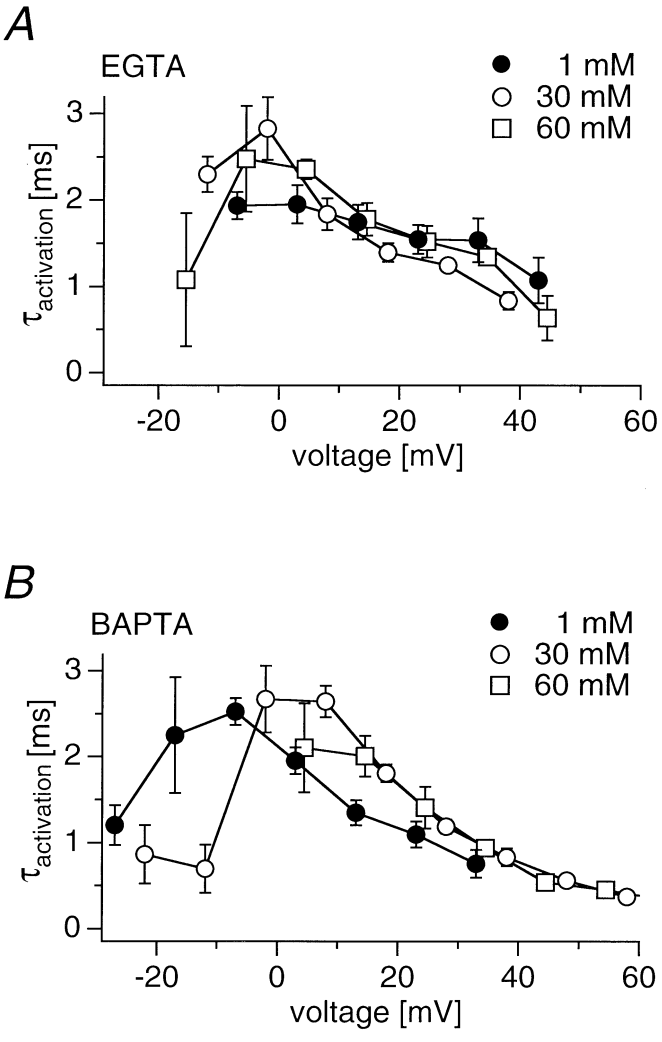

Fig. 3A,B Effects of BAPTA or EGTA on Ca^{2+} current activation kinetics. **A** Average activation time constants of Ca^{2+} currents as measured from cells perfused with standard internal solution supplemented with either 1 mM (●; *n*=4), 30 mM (○; *n*=4), or 60 mM EGTA (□; *n*=5) and plotted versus voltage. **B** Average activation time constants of Ca^{2+} currents as measured from cells perfused with either 1 mM (●; *n*=7), 30 mM (○; *n*=6), or 60 mM BAPTA (□; *n*=8) and plotted versus voltage

Although we took great care to avoid "artefactual" shifts in voltage dependence induced by LJP errors, there is of course the concern that non-specific actions might contribute to the observed effects. If high concentrations of BAPTA somehow altered the general voltage sensitivity of voltage-gated ion channels in an unspecific manner, then not only Ca^{2+} currents but other voltage-dependent currents should also be altered. We probed for such a possibility by determining the voltage dependence of voltage-operated Na^+ channels. However, we did not observe any major effects of BAPTA at concentrations of 1, 10, and 60 mM on the current-voltage relationships of Na^+ currents (Fig. 4). V_{half} remained stable at –16 mV with all three concentrations tested, although E_{rev} increased from +50±0.3 mV for 1 mM to +60±2.3 mV for 60 mM BAPTA (see Table 4). Therefore, the previously described effects of BAPTA seem fairly specific for Ca^{2+} channels and do not result from a general alteration in the voltage sensitivity of all ion channels.

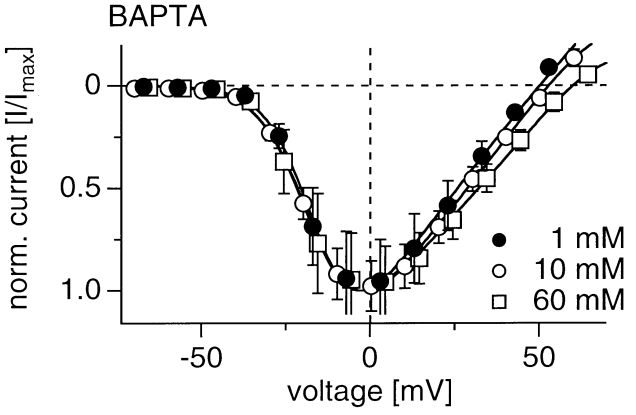

Fig. 4 Effects of BAPTA on the voltage dependence of Na^+ currents. Average current-voltage relationship taken from cells perfused with standard internal solution supplemented with either 1 mM (●; *n*=6), 10 mM (○; *n*=5), or 60 mM BAPTA (□; *n*=5). Current amplitudes were determined in the same manner as Ca^{2+} currents, normalized to I_{max} and plotted versus voltage

Table 3 Effects of BAPTA on current-voltage parameters of Ba^{2+} currents. Values represent parameters derived from fits to averaged current-voltage relationships

Chelator	Concentration (mM)	V_{half} (mV)	Slope (mV)	E_{rev} (mV)	I_{max} (pA/pF)	*n*
BAPTA	1	–6.0	5.0	55.3	–70.0±13.3	5
	60	2.4	5.0	59.1	–61.1±5.7	5

Table 4 Effects of BAPTA on current-voltage parameters of Na^+ currents. All values are means ±SEM and represent averaged parameters derived from fits to current-voltage relationships of individual cells

Chelator	Concentration (mM)	V_{half} (mV)	Slope (mV)	E_{rev} (mV)	I_{max} (pA/pF)	*n*
BAPTA	1	–15.2±0.4	6.8±1.2	50.3±0.3	–97.0±24.7	6
	10	–15.9±0.2	7.3±1.3	52.9±1.7	–60.1±7.9	5
	60	–16.8±0.6	7.1±3.7	60.1±2.3	–107.2±22.1	5

In a series of additional experiments, we set out to investigate whether the BAPTA-related effects on Ca^{2+} currents were mediated by indirect actions through signalling mechanisms that are known to influence Ca^{2+} channel properties.

Interactions with PKC

In bovine adrenal chromaffin cells, Ca^{2+} channels are modulated by PKC [33]. In order to test whether the BAPTA effects are mediated via PKC, we carried out experiments with known activators and inhibitors of this enzyme. In particular, we were probing for the ability of any of the PKC modulators to induce the prominent shift in the activation curve of the Ca^{2+} channels toward positive potentials. These experiments were all carried out in the presence of intracellular EGTA (which by itself does not induce major alterations of the current-voltage parameters) and subsequent extracellular application of the various pharmacological agents. The selective PKC inhibitor bisindolylmaleimide was applied at a concentration of 500 nM [34]. The PKC inhibitor staurosporine was used at fairly high concentrations of 2 or 50 µM from the extracellular space. At such high concentrations other kinases such as tyrosine kinases, cAMP- and cGMP-dependent protein kinases, Ca^{2+}-calmodulin dependent protein kinase, and myosin light-chain kinase are also blocked [32]. Finally, the phorbol ester phorbol-12-myristate-13-acetate (PMA) was used at a concentration of 100 nM to stimulate PKC activity [25].

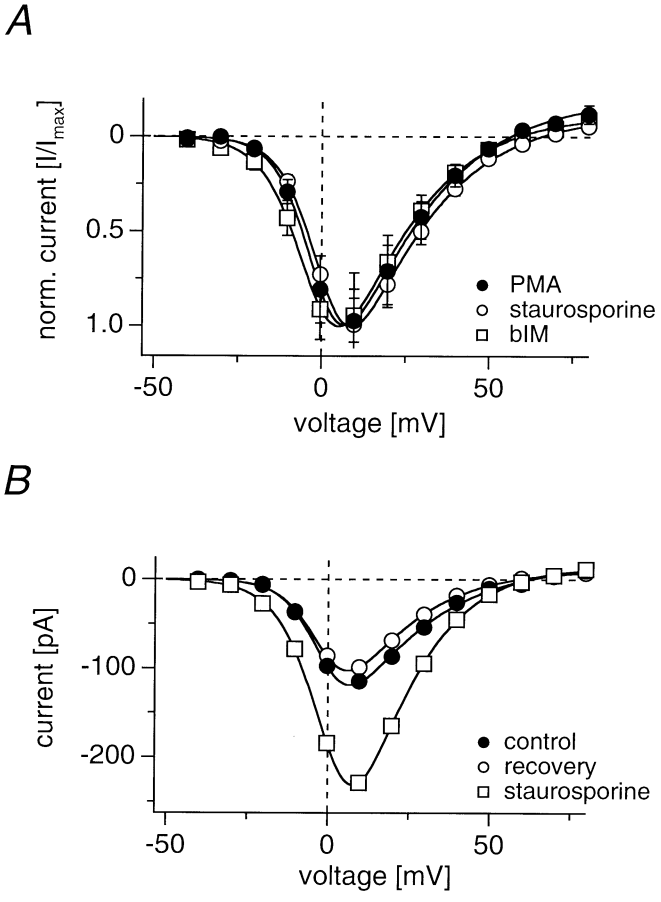

Fig. 5A,B Interactions between BAPTA and protein kinase C. **A** Average Ca^{2+} current-voltage relationship taken from cells superfused with external Ringer solution supplemented with either PMA (●; *n*=4), staurosporine (○; *n*=6), or bisindolylmaleimide (□; *n*=4). **B** Current-voltage relationships taken from a single cell before (●), during extracellular application of staurosporine (□), and after washout of the compound (○)

Figure 5A shows the current-voltage relationships for experiments in the presence or absence of the substances mentioned above. To facilitate the detection of changes in the voltage dependence, the currents were normalized to their fitted peak values. None of these treatments were able to mimic the BAPTA-mediated shift of the current-voltage curve to more positive potentials (see also Table 3). Likewise, there was no obvious effect of either 50 µM staurosporine or 500 nM bisindolylmaleimide when administered intracellularly (data not shown). Thus it seems unlikely that BAPTA affects Ca^{2+} currents indirectly by stimulating or inhibiting PKC.

It should be noted, however, that during staurosporine or bisindolylmaleimide application there was a reversible increase in the peak current amplitude and faster activation kinetics (Fig. 5B). This phenomenon was seen in three out of four cells exposed to staurosporine and two out of four cells treated with bisindolylmaleimide. In one out of four cells stimulated with PMA, the peak current amplitude decreased and the activation time constant decreased (data not shown). These results are in good agreement with the ones described by Sena et al. [33], who reported a PMA-induced inhibition of voltage-sensitive Ca^{2+} channels in adrenal chromaffin cells. The averaged amplitudes of Ca^{2+} currents, however, were not significantly different in the presence of these drugs (see Table 5). This might be due to cell variability and the fact that the augmentation/reduction of Ca^{2+} currents was not seen in all cells.

Table 5 Effects of kinase activators/inhibitors on current-voltage parameters of Ca^{2+} currents. Standard internal solution was buffered with 10 mM EGTA. Values represent parameters derived from fits to averaged current-voltage relationships

Compound	Concentration	V_{half} (mV)	Slope (mV)	E_{rev} (mV)	I_{max} (pA/pF)	*n*
Phorbol ester	100 nM	0.5	5.3	56.2	–51.7	4
Staurosporine	2 µM	2.0	5.4	64.3	–49.9	6
	50 µM	0.8	5.7	51.2	–40.7	5
Bisindolylmaleimide	500 nM	–0.9	5.9	58.5	–83.4	4

Interactions with G proteins

In many cells, including chromaffin cells [18], heterotrimeric G-proteins cause a shift in the current-voltage relationship to more positive potentials and a decrease in peak current amplitude [4]. It is therefore possible that BAPTA might either mimic directly or stabilize G-protein-mediated actions indirectly. This was tested in experiments with stimulatory and inhibitory GTP analogues. Guanosine 5'-*O*-(2-thiodiphosphate) (GDP[β-*S*]) is an irreversible blocker of G-protein activity, while GTP[γ-*S*] has the opposite effect [12]. The efficacy of the GTP analogues was first verified by experiments carried out in the presence of 10 mM EGTA, which reliably yielded augmentation of Ca^{2+} current amplitudes by GDP[β-*S*] and a strong suppression by GTP[γ-*S*] (see Table 6). The V_{half} values for the combination of GDP[β-*S*] and EGTA (Table 6) were consistently more positive than the controls with EGTA alone (see Table 2), but did not significantly change even when 60 mM EGTA was added to the GDP[β-*S*]-containing solution. Interestingly, the V_{half} values for the combination of GTP[γ-*S*] and EGTA was not very different from the GDP[β-*S*]+EGTA combination. In fact, higher EGTA concentrations caused a moderate shift of V_{half} toward less positive potentials (Table 6). Thus, the presence of either GTP analog produced fairly positive V_{half} values when EGTA was used as the chelator.

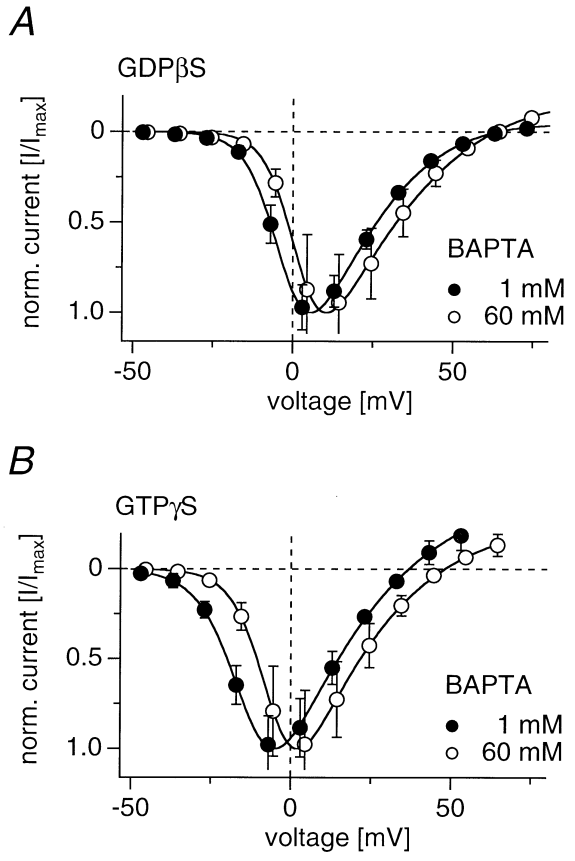

Fig. 6A,B Interactions between BAPTA and G proteins. **A** Average Ca^{2+} current-voltage relationship derived from cells perfused with standard internal solution supplemented with GDP[β-*S*] and either 1 mM (●; *n*=4) or 60 mM BAPTA (○; *n*=4). **B** Mean current-voltage relationship obtained from cells perfused with standard internal solution supplemented with GTP[γ-*S*] and either 1 mM (●; *n*=4) or 60 mM BAPTA (○; *n*=4)

The next set of experiments was carried out by including the GTP analogs and BAPTA in the pipette solution. The current-voltage relationships obtained with GDP[β-*S*] and 1 or 60 mM BAPTA are shown in Fig. 6A. As can be seen, V_{half} was more negative than the corresponding value obtained with GDP[β-*S*]+EGTA, but the shift in voltage sensitivity induced by high concentrations of BAPTA was still present under these conditions, although to a lesser degree. V_{half} was changed by 4 mV towards positive potentials, while E_{rev} stayed constant at about 63 mV (see Table 6). When using GTP[γ-*S*], a transient Cl^- conductance was activated in all cells tested (data not shown). This transient current has been described previously by Doroshenko et al. [11]. The recording of the Ca^{2+} current was started after the Cl^- current decayed, which was usually the case after about 5 min. Again, V_{half} was more negative than the corresponding value obtained with GDP[β-*S*]+EGTA, even at the higher BAPTA concentration. Nevertheless, the current-voltage curve with 60 mM BAPTA was shifted by 7 mV to more positive voltages compared to the one recorded with 1 mM BAPTA (Fig. 6B, Table 6).

These results point towards a possible involvement of G proteins in the mediation of BAPTA's effects, at least

Table 6 Effects of GTP analogs and chelators on current-voltage parameters of Ca^{2+} currents. BAPTA values are means ±SEM and represent averaged parameters derived from fits to current-voltage relationships of individual cells. EGTA values are parameters of fits to averaged current-voltage relationships

Compound	Concentration (mM)	V_{half} (mV)	Slope (mV)	E_{rev} (mV)	I_{max} (pA/pF)	*n*
GDP[β-*S*]/BAPTA	0.5/1	–2.1±1.6	5.1±0.7	63.6±1.6	–76.2±8.9	4
	0.5/60	2.4±1.4	5.1±0.2	62.9±1.4	–59.5±17.9	4
GTP[γ-*S*]/BAPTA	0.2/1	–12.0±1.6	6.1±0.3	39.1±3.3	–13.5±2.3	4
	0.2/60	–4.7±2.0	5.1±0.7	47.3±2.0	–27.0±8.3	4
GDP[β-*S*]/EGTA	0.5/1	12.3	4.8	68.4	–134.1	4
	0.5/10	10.1	5.5	68.0	–101.5	4
	0.5/60	10.5	5.5	72.3	–140.2	4
GTP[γ-*S*]/EGTA	0.2/1	8.9	5.1	55.7	–107.8	5
	0.2/10	6.3	6.4	63.0	–48.9	4
	0.2/60	2.2	6.3	58.0	–90.2	4

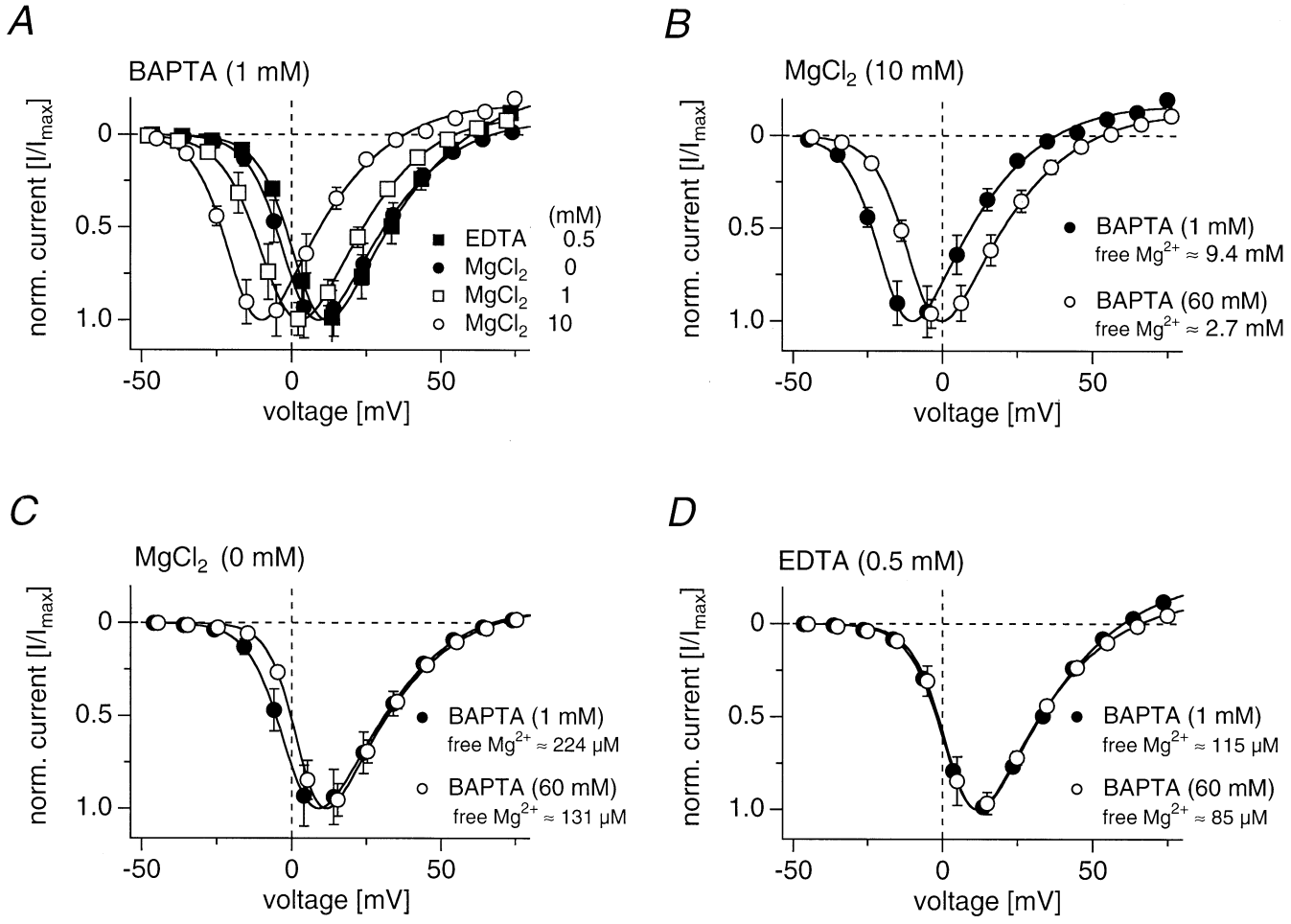

Fig. 7A–D Interactions between BAPTA and $[Mg^{2+}]_i$. **A** Average Ca^{2+} current-voltage relationship derived from cells perfused with standard internal solution supplemented with 1 mM BAPTA and either 0.5 mM EDTA (■; *n*=5), 0 mM Mg^{2+} (●; *n*=5), 1 mM Mg^{2+} (□; *n*=5) or 10 mM Mg^{2+} (○; *n*=5). **B** Average current-voltage relationship obtained from cells perfused with standard internal solution supplemented with 10 mM Mg^{2+} and either 1 mM BAPTA (●; *n*=5) or 60 mM BAPTA (○; *n*=5). **C** Mean current-voltage relationship derived from cells perfused with standard internal solution with no added Mg^{2+} and supplemented with either 1 mM BAPTA (●; *n*=5) or 60 mM BAPTA (○; *n*=5). **D** Average current-voltage relationship obtained from cells perfused with standard internal solution supplemented with 0.5 mM EDTA and either 1 mM BAPTA (●; *n*=5) or 60 mM BAPTA (○; *n*=5)

partially, since both GDP[β-*S*] and GTP[γ-*S*] attenuated the BAPTA effects to some extent. However, modulation of G protein's actions cannot account entirely for the actions of BAPTA, as the general tendency of BAPTA to shift the voltage sensitivity of Ca^{2+} currents remained evident.

Interactions with $[Mg^{2+}]_i$

Both BAPTA and EGTA are characterized by a more than a 10,000-fold higher selectivity in chelating Ca^{2+} over Mg^{2+}. Nevertheless, we tested whether part of the BAPTA effect was related to its Mg^{2+} binding when high concentrations of BAPTA were used. These experiments were carried out with either 1 mM or 60 mM $[BAPTA]_i$ and varying the free internal Mg^{2+} concentration between 9.4 mM and approximately zero by adding various amounts of $MgCl_2$ and EDTA (a less specific divalent chelator) to the standard internal solution.

In the previous experiments, the standard intracellular solutions always contained 1 mM $MgCl_2$ (and the standard 4 mM Mg-ATP), which in the presence of 1 mM BAPTA translates to 824 µM free $[Mg^{2+}]_i$ and is reduced to 285 µM in the presence of 60 mM BAPTA. To assess the effects of various concentrations of $MgCl_2$, we chose to use a fixed BAPTA concentration of 1 mM, which causes only a small drop in free $[Mg^{2+}]_i$ and does not cause a significant right-shift in the current-voltage curves. Figure 7A shows the current-voltage relationships, recorded with 1 mM BAPTA and free $[Mg^{2+}]_i$ between 115 µM and 9.4 mM. It is seen that variations in Mg^{2+} cause striking changes in the current-voltage relationship of Ca^{2+} currents. Increasing free $[Mg^{2+}]_i$ to 9.4 mM (by including 10 mM $MgCl_2$ in the pipette solution) shifted V_{half} to –17 mV, whereas decreasing $[Mg^{2+}]_i$ to 0.824 mM (1 mM added $MgCl_2$) and 0.224 mM $[Mg^{2+}]_i$ (0 added $MgCl_2$) shifted V_{half} to –5 mV and +1 mV, respectively. A further reduction in free $[Mg^{2+}]_i$ to 0.115 mM was accomplished by adding EDTA, which resulted in a further shift of the current-voltage curve

Table 7 Effects of $[Mg^{2+}]_i$ and chelators on current-voltage parameters of Ca^{2+} currents. All values are means ±SEM. Values represent averaged parameters derived from fits to current-voltage relationships of individual cells

Compound	Concentration (mM)	V_{half} (mV)	Slope (mV)	E_{rev} (mV)	I_{max} (pA/pF)	*n*
Mg^{2+}/BAPTA	10/1	–16.6±0.2	5.6±0.4	37.7±0.7	–16.2±2.3	5
	10/60	–7.2±0.2	5.6±0.8	52.8±1.9	–52.2±4.7	5
Mg^{2+}/BAPTA	1/1	–4.9±0.1	6.8±1.0	54.5±0.7	–57.2±6.4	5
	1/60	4.6±0.1	5.3±0.5	61.1±1.4	–57.3±4.6	5
Mg^{2+}/BAPTA	0/1	0.8±0.2	5.9±1.0	67.0±2.6	–77.6±12.6	5
	0/60	4.2±0.3	4.7±1.0	69.4±0.6	–161.0±16.5	5
Mg^{2+}/BAPTA	0/1/0.5	4.4±0.7	5.7±0.3	60.0±2.8	–74.6±10.9	5
EDTA	0/60/0.5	4.6±0.9	5.4±0.3	65.6±0.9	–112.7±10.1	5

(V_{half}: +4 mV). Thus, by decreasing the $[Mg^{2+}]_i$ from about 9.4 to 0.115 mM, V_{half} increased from –17 mV to +4 mV. This is a difference of 21 mV between the highest and lowest Mg^{2+} concentration tested (significant at $P<0.01$).

The next series of experiments was designed to assess the efficacy of different BAPTA concentration at inducing the shift in V_{half} under conditions of very high, intermediate, and very low Mg^{2+} concentrations. When 10 mM $MgCl_2$ was added to the pipette solution, an increase in BAPTA from 1 to 60 mM caused a shift in V_{half} of about 10 mV to the right (Fig. 7B). At the same time, the equivalent free $[Mg^{2+}]_i$ was reduced from 9.4 mM to 2.7 mM. Thus, the BAPTA-induced changes in the voltage dependence are still apparent when $[Mg^{2+}]_i$ is relatively high, although to a slightly lesser extent compared with the 15-mV shift observed with 1 mM added $MgCl_2$ (equivalent to 0.824 mM free $[Mg^{2+}]_i$).

Using a Mg^{2+}-free internal solutions (i.e. no added $MgCl_2$, except for the standard 4 mM MgATP), the free $[Mg^{2+}]_i$ was 224 µM (with 1 mM BAPTA) and 131 µM (with 60 mM BAPTA). Under these conditions (Fig. 7C), the current-voltage curve obtained for the high BAPTA concentration showed only a slight change in voltage sensitivity compared to the lower BAPTA concentration (V_{half} was shifted by ≅3 mV to positive potentials). To further reduce the intracellular Mg^{2+} concentration, the unspecific chelator EDTA was added at a concentration of 0.5 mM to the Mg^{2+}-free internal solution. In this solution, the free $[Mg^{2+}]_i$ was decreased to calculated values of 115 µM (in the presence of 1 mM BAPTA) and 85 µM (at 60 mM BAPTA). Now, high concentrations of BAPTA caused no further shift in the voltage sensitivity of the Ca^{2+} currents. The two current-voltage curves are essentially identical (Fig. 7D). The current-voltage parameters of these experiments are summarized in Table 7. Taken together, these data suggest that the free Mg^{2+} concentration appears to have similar effects on the voltage sensitivity of Ca^{2+} channels as BAPTA; low $[Mg^{2+}]_i$ tends to shift the activation curve of Ca^{2+} channels to the right. However, as is discussed later, this does not necessarily suggest that BAPTA exerts its effects by simply reducing the free $[Mg^{2+}]_i$.

A few additional observations that deserve more detailed study in the future are noteworthy. The values of E_{rev} shifted from 60, 55 to 38 mV, when internal solutions with free $[Mg^{2+}]_i$ of 0.115, 0.824 and 9.4 mM were used. The E_{rev} values of 60 and 38 mV differ significantly ($P<0.01$). These data could suggest that internal Mg^{2+} may affect Ca^{2+} channel selectivity, possibly by acting as a charge carrier.

Another observation was that the peak current amplitude decreased with increasing $[Mg^{2+}]_i$. With 115 and 224 µM free $[Mg^{2+}]_i$, the Ca^{2+} current peaked at about –76 pA/pF. When $[Mg^{2+}]_i$ was increased to 824 µM, the current density decreased to a value of about –58 pA/pF and with 9.4 mM free $[Mg^{2+}]_i$, the peak current was reduced to only –16 pA/pF. This might indicate that internal Mg^{2+} is able to block voltage-dependent Ca^{2+} influx.

Furthermore, in the experiments where the $[Mg^{2+}]_i$ was kept very low by adding EDTA, a Cl^- current similar to the GTP[γ-*S*]-activated Cl^- conductance activated and inactivated spontaneously in all cells. The same current was also recorded when the internal solution without added $MgCl_2$ was used (32 of 33 cells for 1 mM BAPTA and all 12 cells for 60 mM BAPTA). However, in Rat Basophilic Leukemia cells (RBL-2H3), Chinese Hamster Ovary cells (CHO) and hippocampal neurons no such current was recorded under identical ionic conditions. Therefore, the lack of $[Mg^{2+}]_i$ is not sufficient to activate Cl^- currents as a general mechanism in a wide variety of cell types and may represent a special feature of chromaffin cell Cl^- channels.

Discussion

The results of this study clearly establish that EGTA and BAPTA can have different effects on the voltage-operated Ca^{2+} currents in bovine adrenal chromaffin cells: (1) increasing concentrations of BAPTA from 1 to 60 mM caused a 15-mV shift in the voltage sensitivity of Ca^{2+} currents toward more positive potentials, a phenomenon that was not seen when EGTA was tested over the same concentration range; (2) the current amplitudes were generally larger when high concentrations of BAPTA were used, whereas EGTA did not show a concentration-dependent effect on peak current amplitudes. While the latter effect might be related to BAPTA's faster Ca^{2+} buffering as compared to EGTA (but see discussion below), the effects on voltage dependence are not easily explained by a simple difference in Ca^{2+}-binding kinetics

(which is the main difference between the two chelators; the dissociation constants and hence the total buffering efficacy of both chelators are quite similar).

Both chelators were used in their highest purity grade (see Materials and methods). Since both chelators were used at a concentration as high as 60 mM, possible impurities could have been present at a maximum of 0.6 mM. Therefore, it can not be completely ruled out that a contaminating substance might have been responsible for the effects described here. On the other hand, Harrison and Bers [16] reported that most of the impurities in Ca^{2+} chelators are due to water content. Regardless of this, investigators need to be aware that commercial batches of BAPTA might affect Ca^{2+} currents in the way described in this study.

The main effect of BAPTA was to alter the voltage dependence of Ca^{2+} currents such that increasing concentrations from 1 to 60 mM shifted V_{half} by about 15 mV in the depolarizing direction. The alterations in the voltage dependence take place over a concentration range, which is often used by electrophysiologists. It should be noted, that the shift of the current-voltage curve is even more prominent (almost 25 mV) when neglecting to carefully correct for LJPs (amounting to 9 mV between 1 and 60 mM BAPTA). A second observation relates to peak current amplitudes, which were larger with BAPTA as compared to EGTA. There are several reasons that seem to rule out a simple explanation of these effects in terms of Ca^{2+}-buffering properties of the two chelators:

1. Both chelators have similar effective dissociation constants (around 150–200 nM).
2. BAPTA's faster Ca^{2+} buffering compared to EGTA may not be a relevant factor here, since, regardless of the chelator or the concentration used, there was no evidence of Ca^{2+}-dependent inactivation of Ca^{2+} currents in chromaffin cells. This is in good agreement with the observations of Marty and Neher [22], who also reported remarkably stable current amplitudes over an EGTA concentration range of 0.5 to 10 mM.
3. Even when clamping intracellular free Ca^{2+} concentration to resting levels of about 100 nM by appropriate mixtures of Ca^{2+} and BAPTA, high total buffer concentrations still caused the shift to occur (data not shown). It would therefore appear that BAPTA might either directly or indirectly interfere with the Ca^{2+} channels through some process that regulates the voltage sensitivity of the channels.

The major mechanism known to affect Ca^{2+} channel gating is through G proteins. It is well established that N-type Ca^{2+} channels can be inhibited by activation of G proteins, presumably through interaction with $G\beta\gamma$ subunits [10]. As a result, in many cellular systems, Ca^{2+} channels exhibit a shift in their voltage-activation curve towards positive potentials. The situation is not as clear-cut in chromaffin cells, since chromaffin cells possess a mixture of different Ca^{2+} channels; including N- and P/Q-type [2, 3]. Also, the most prominent effect of GTP[γ-*S*] in chromaffin cells is not a shift in the activation curve, but rather a strong reduction in current amplitude. Our present results indicate that there may indeed be some interaction of BAPTA with G-protein-induced modulation of Ca^{2+} channels, as BAPTA was less effective in shifting the voltage dependence of Ca^{2+} currents when either GTP[γ-*S*] or GDP[β-*S*] were perfused into the cells. Clearly, the BAPTA effects are not simply a stabilization of the G-protein-bound state, nor does BAPTA seem to mimic the G protein inhibition, since current amplitudes were not reduced (as is always the case with GTP[γ-*S*]). Since G proteins are thought to directly bind to Ca^{2+} channels, the interaction between BAPTA and G proteins indicates that BAPTA might also interact directly with the Ca^{2+} channels.

Intracellular Mg^{2+} has been shown to block Ca^{2+} channels [20]. This blocking effect seems to be different for different Ca^{2+} channel types, with a fairly selective inhibition of the ω-conotoxin-GVIA-sensitive component of Ca^{2+} current in rat cerebellar granule cells [27]. Although BAPTA and EGTA are fairly selective Ca^{2+} chelators with rather low affinities for Mg^{2+}, our results indicate that free $[Mg^{2+}]_i$ is an important determinant of the voltage dependence of activation as well as Ca^{2+} current amplitude in chromaffin cells. Low $[Mg^{2+}]_i$ causes a shift of the activation curve towards positive potentials and at the same time increases peak current amplitudes. Increasing $[Mg^{2+}]_i$ has the opposite effect. A direct interaction between Mg^{2+} and the Ca^{2+} channels might explain this behavior. Cell membranes are negatively charged, so that cations such as Mg^{2+} are attracted. The charge will be sensed depending on its distance to the voltage sensor of Ca^{2+} channels so that the gating behavior is altered [14, 17]. At low Mg^{2+} concentrations, the voltage sensor would "see" a more negative membrane potential. This would mean that stronger depolarizations are necessary to open the pore. As a result the voltage dependence would be shifted to more positive potentials, as is measured experimentally. Thus, $[Mg^{2+}]_i$ seems to mimic the BAPTA effects in a reciprocal manner. It is particularly interesting that the $[Mg^{2+}]_i$-induced modulations of voltage-operated Ca^{2+} current occur over a concentration range that indeed exists under in vivo conditions [19].

Could BAPTA's effects be mediated by chelation of Mg^{2+}? This seems unlikely, since BAPTA's affinity for Mg^{2+} is very similar to that of EGTA, yet EGTA fails to produce similar effects. However, since Mg^{2+} is likely to exert its effects by directly binding to the inner mouth of the Ca^{2+} channels, it may be an indication that both Mg^{2+} and BAPTA compete for that site. In this scenario, BAPTA might displace Mg^{2+} from the Ca^{2+} channels, resulting in an apparent lowering of local $[Mg^{2+}]_i$ at the Ca^{2+} channels. This may then result in a shift of the activation curve as well as an increase in Ca^{2+} current amplitude. Alternatively, BAPTA might cause its effects indirectly by binding to another protein that in turn increases its affinity for Mg^{2+}, thereby reducing free $[Mg^{2+}]_i$ and leading to increased Ca^{2+} currents as well as shifts in the current-voltage relationship.

A further interesting observation was that another divalent ion (namely Ba^{2+}) partially suppressed the BAPTA-induced shift in the current-voltage curve (Table 3). Although we have no full understanding of this effect, it could indicate that the Ca^{2+}-bound form of BAPTA might be more effective at exerting the shift than the Ba^{2+}-bound species.

In conclusion, from the findings presented here, one needs to be aware of or at least consider undesirable effects of chelators like BAPTA, which are not simply related to their Ca^{2+}-binding properties. At least in bovine adrenal chromaffin cells, BAPTA but not EGTA shifts the voltage sensitivity of Ca^{2+} currents and affects current size. The mechanism by which BAPTA induces these effects seems to be complex, because G proteins and the free intracellular concentration of Mg^{2+} appear to be involved. Whether other Ca^{2+} influx pathways in both excitable and non-excitable cells are also influenced by chelators remains to be determined.

References

1. Albillos A, Garcia AG, Gandia L (1993) Omega-Agatoxin-IVA-sensitive calcium channels in bovine chromaffin cells. FEBS Lett 336:259–262
2. Albillos A, Garcia AG, Olivera B, Gandia L (1996) Re-evaluation of the P/Q Ca^{2+} channel components of Ba^{2+} currents in bovine chromaffin cells superfused with solutions containing low and high Ba^{2+} concentrations. Pflügers Arch 432:1030–1038
3. Artalejo C, Mogul DJ, Perlma RL, Fox AP (1991) Three types of bovine chromaffin cell Ca^{2+} channels: facilitation increases the opening probability of a 27 pS channel. J Physiol (Lond) 444:213–240
4. Bean BP (1989) Neurotransmitter inhibition of neuronal calcium currents by changes in channel voltage-dependence. Nature 340:153–155
5. Beech DJ, Bernheim L, Hille B (1992) Pertussis toxin and voltage dependence distinguish muliple pathways modulating calcium channels of rat sympathetic neurons. Neuron 8:97–106
6. Beech DJ, Bernheim L, Mathie A, Hille B (1991) Intracellular Ca^{2+} buffers disrupt muscarinic suppression of the Ca^{2+} current and M current in rat sympathetic neurons. Proc Natl Acad Sci USA 88:652–656
7. Bernheim L, Beech DJ, Hille B (1991) A diffusible second messenger mediates one of the pathways coupling receptors to calcium channels in rat sympathetic neurons. Neuron 6:859–867
8. Bödding M, Penner, R (1995) Pharmacological effects of Ca^{2+} chelators on Ca^{2+} currents in bovine chromaffin cells (abstract). Pflügers Arch 429:35 R 21
9. Coorssen JR, Haslam RJ (1993) GTP[γ-*S*] and phorbol ester act synergistically to stimulate both Ca^{2+}-independent secretion and phospholipase D activity in permeabilized human platelets. FEBS Lett 316:170–174
10. Dolphin AC (1998) Mechanisms of modulation of voltage-dependent calcium channels by G-proteins. J Physiol (Lond) 506:3–11
11. Doroschenko P, Penner R, Neher E (1991) Novel chloride conductance in the membrane of bovine chromaffin cells activated by intracellular GTPγ S. J Physiol (Lond) 436:711–724
12. Eckstein F (1985) Nucleoside phosphorothioates. Annu Rev Biochem 54:367–402
13. Fenwick EM, Marty A, Neher E (1982) A patch-clamp study of bovine chromaffin cells and of their sensitivity to acetylcholine. J Physiol (Lond) 331:577–597
14. Frankenhaeuser B, Hodgkin AL (1957) The action of calcium on the electrical properties of the squid axons. J Physiol (Lond) 137:218–244
15. Hamill OP, Marty A, Neher E, Sakmann B, Sigworth FJ (1981) Improved patch-clamp techniques for high resolution current recording from cells and cell-free membrane patches. Pflügers Arch 391:85–100
16. Harrison SM, Bers DM (1987) The effect of temperature and ionic strength on the apparent Ca-affinity of EGTA and the analogous Ca-chelators BAPTA and dibromo-BAPTA. Biochim Biophys Acta 925:133–143
17. Hille B (1992) Ionic channels of excitable membranes, 2nd edn. Sinauer, Sunderland, Mass., USA
18. Hille B (1994) Modulation of ion-channel function by G-protein-coupled receptors. Trends Neurosci 17:531–535
19. Kelepouris E, Kasama R, Agus ZS (1993) Effects of intracellular magnesium on calcium and chloride channels. Miner Electrolytes Metab 19:277–281
20. Kuo CC, Hess P (1993) Block of the L-type Ca^{2+} channel pore by external and internal Mg in rat phaeochromocytoma cells. J Physiol (Lond) 466:683–706
21. Martell AE, Smith RM (1979) Critical stability constants. Amino acids, Vol. 1, Plenum, New York
22. Marty A, Neher E (1985) Potassium channels in cultured bovine adrenal chromaffin cells. J Physiol (Lond) 367:117–141
23. Morris SM, Correa V, Cardy TJA, O'Beirne G, Taylor CW (1999) Interactions between inositol trisphosphate receptors and the fluorescent Ca^{2+} indicators. Cell Calcium 25:137–142
24. Neher E (1992) Correction for liquid junction potentials in patch clamp experiments. In: Rudy B, Iverson LE (eds) Methods in enzymology, Vol. 207, Ion channels. Academic, San Diego, Calif., USA, pp 123–131
25. Nishizuka Y (1988) The molecular heterogeneity of protein kinase C and its implications for cellular regulation. Nature 334:661–665
26. Parekh AB, Penner R (1995) Depletion-activated calcium current is inhibited by protein kinase in RBL-2H3 cells. Proc Natl Acad Sci USA 92:7907–7911
27. Pearson HA, Campbell V, Berrow N, Menon-Johannsson A, Dolphin AC (1994) Modulation of voltage-dependent calcium channels in cultured neurons. Ann NY Acad Sci 747:323–335
28. Pelzer D, Pelzer S, McDonald TF (1990) Properties and regulation of calcium channels in muscle cells. Rev Physiol Biochem Pharmacol 114:107–207
29. Penner R, Neher E (1988) Secretory response of rat peritoneal mast cells to high intracellular calcium. FEBS Lett 226:307–313
30. Pusch M, Neher E (1988) Rates of diffusional exchange between small cells and a measuring patch pipette. Pflügers Arch 411:204–211
31. Richardson A, Taylor CW (1993) Effects of Ca^{2+} chelators on purified inositol 1,4,5-trisphosphate ($InsP_3$) receptors and $InsP_3$-stimulated Ca^{2+} mobilisation. J Biol Chem 268:11528–11533
32. Rüegg UT, Burgess GM (1989) Staurosporine, K-252 and UCN-01: potent but nonspecific inhibitors of protein kinases. Trends Pharmacol Sci 10:218–220
33. Sena CM, Tome AR, Santos RM, Rosario LM (1995) Protein kinase C activator inhibits voltage-sensitive Ca^{2+} channels and catecholamine secretion in adrenal chromaffin cells. FEBS Lett 359:137–141
34. Toulles D, Pianetti P, Coste H, Belleveergue P, Grand-Perret T, Ajakane M, Baudet V, Boissin P, Boursier R, Loriolle F, Duhamel L, Charon D, Kirilovsky J (1991) The bisindolylmaleimide GF 109203X is a potent and selective inhibitor of protein kinase C. J Biol Chem 266:15771–15781
35. Tsien RY (1980) New calcium indicators and buffers with high selectivity against magnesium and protons: design, synthesis and prototype structures. Biochemistry 19:2396–2404
36. Yue DT, Backx PH, Imredy JP (1990) Calcium-sensitive inactivation in the gating of single calcium channels. Science 250: 1735–1738